

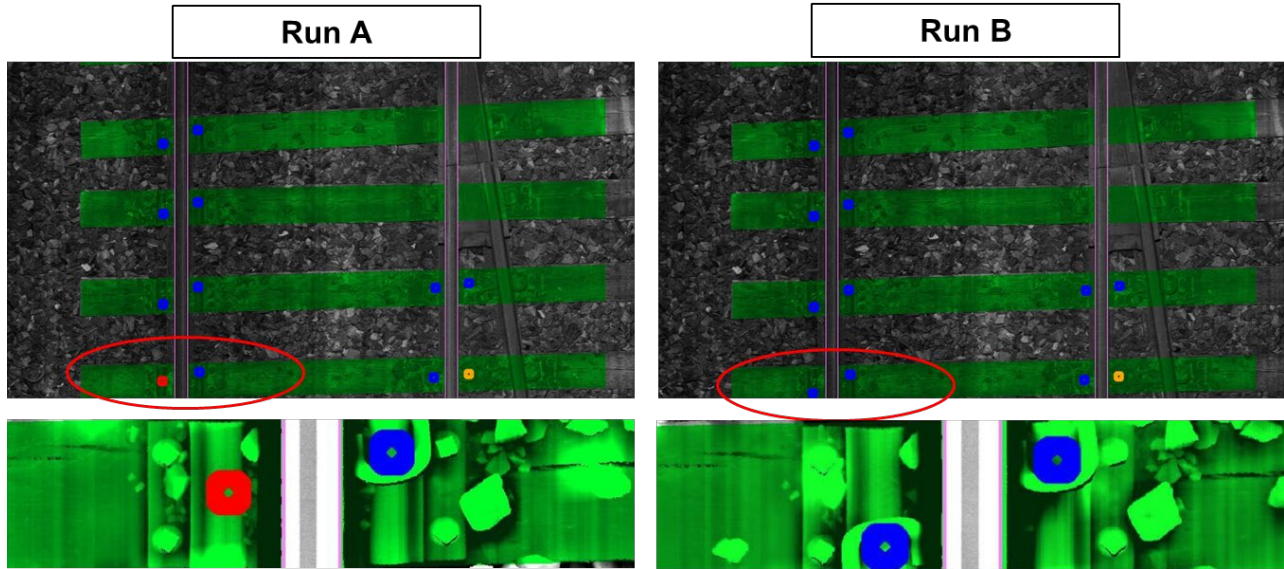


U.S. Department of  
Transportation

**Federal Railroad  
Administration**

# Laser Triangulation for Track Change and Defect Detection

Office of Research,  
Development  
and Technology  
Washington, DC 20590



#### NOTICE

This document is disseminated under the sponsorship of the Department of Transportation in the interest of information exchange. The United States Government assumes no liability for its contents or use thereof. Any opinions, findings and conclusions, or recommendations expressed in this material do not necessarily reflect the views or policies of the United States Government, nor does mention of trade names, commercial products, or organizations imply endorsement by the United States Government. The United States Government assumes no liability for the content or use of the material contained in this document.

#### NOTICE

The United States Government does not endorse products or manufacturers. Trade or manufacturers' names appear herein solely because they are considered essential to the objective of this report.

<b>REPORT DOCUMENTATION PAGE</b>			<i>Form Approved</i> <i>OMB No. 0704-0188</i>	
Public reporting burden for this collection of information is estimated to average 1 hour per response, including the time for reviewing instructions, searching existing data sources, gathering and maintaining the data needed, and completing and reviewing the collection of information. Send comments regarding this burden estimate or any other aspect of this collection of information, including suggestions for reducing this burden, to Washington Headquarters Services, Directorate for Information Operations and Reports, 1215 Jefferson Davis Highway, Suite 1204, Arlington, VA 22202-4302, and to the Office of Management and Budget, Paperwork Reduction Project (0704-0188), Washington, DC 20503.				
1. AGENCY USE ONLY (Leave blank)		2. REPORT DATE March 2020		3. REPORT TYPE AND DATES COVERED Technical Report, March 2017 – December 2017
4. TITLE AND SUBTITLE Laser Triangulation for Track Change and Defect Detection			5. FUNDING NUMBERS DTFR53-17-C-00005	
6. AUTHOR(S) Richard Fox-Ivey, Thanh Nguyen, John Laurent				
7. PERFORMING ORGANIZATION NAME(S) AND ADDRESS(ES) Pavemetrics Systems, Inc. 150 boul. Rene-Levesque, suite 1820 Quebec, Canada G1R 5B1			8. PERFORMING ORGANIZATION REPORT NUMBER	
9. SPONSORING/MONITORING AGENCY NAME(S) AND ADDRESS(ES) U.S. Department of Transportation Federal Railroad Administration Office of Railroad Policy and Development Office of Research, Development and Technology Washington, DC 20590			10. SPONSORING/MONITORING AGENCY REPORT NUMBER  DOT/FRA/ORD-20/08	
11. SUPPLEMENTARY NOTES COR: Cameron Stuart				
12a. DISTRIBUTION/AVAILABILITY STATEMENT This document is available to the public through the FRA <a href="#">website</a> .			12b. DISTRIBUTION CODE	
13. ABSTRACT (Maximum 200 words) Pavemetrics Systems Inc. teamed with Amtrak to demonstrate the feasibility of automated track change detection using its Laser Rail Inspection System (LRAIL). LRAIL is a rail inspection system based on the principle of laser triangulation and combines pulsed high-power, invisible, laser line projectors and synchronized cameras to capture a high-resolution-intensity image and 3-dimensional range profile of the railway trackbed. In this project, LRAIL was mounted on a hi-rail testing vehicle and tested at Amtrak's Bear, DE facility and on mainline track.  The LRAIL system includes a library of computer algorithms designed to make automatic measurements, inventory features, and detect changes in trackbed infrastructure. Pavemetrics researchers used algorithms to record and detect changes in fasteners, anchors, spikes, ties, joints, and ballast—as well as record rail manufacturing information. Field validation included the comparison of manual inspections with manual inspections considered "ground-truth." The primary outcome of this project was field-validated evidence of the technology's ability to automatically detect changes in the track structure and highlight these changes for review and possible action.				
14. SUBJECT TERMS Laser triangulation, algorithms, change detection, safety, operational efficiency, inspection			15. NUMBER OF PAGES 32	
			16. PRICE CODE	
17. SECURITY CLASSIFICATION OF REPORT Unclassified	18. SECURITY CLASSIFICATION OF THIS PAGE Unclassified	19. SECURITY CLASSIFICATION OF ABSTRACT Unclassified	20. LIMITATION OF ABSTRACT	

NSN 7540-01-280-5500

Standard Form 298 (Rev. 2-89)  
Prescribed by  
ANSI Std. Z39-18  
298-102

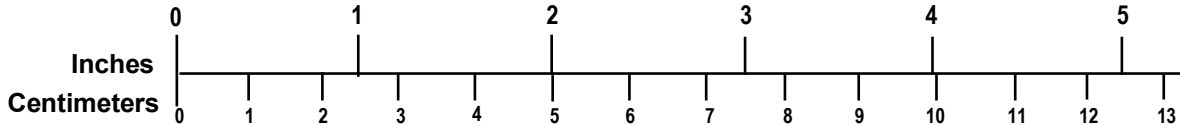
# METRIC/ENGLISH CONVERSION FACTORS

## ENGLISH TO METRIC

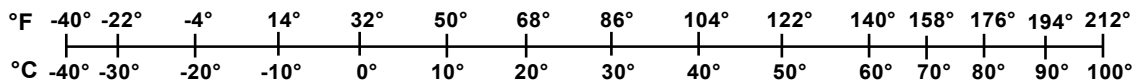
## METRIC TO ENGLISH

<p><b>LENGTH (APPROXIMATE)</b></p> <p>1 inch (in) = 2.5 centimeters (cm)</p> <p>1 foot (ft) = 30 centimeters (cm)</p> <p>1 yard (yd) = 0.9 meter (m)</p> <p>1 mile (mi) = 1.6 kilometers (km)</p>	<p><b>LENGTH (APPROXIMATE)</b></p> <p>1 millimeter (mm) = 0.04 inch (in)</p> <p>1 centimeter (cm) = 0.4 inch (in)</p> <p>1 meter (m) = 3.3 feet (ft)</p> <p>1 meter (m) = 1.1 yards (yd)</p> <p>1 kilometer (km) = 0.6 mile (mi)</p>
<p><b>AREA (APPROXIMATE)</b></p> <p>1 square inch (sq in, in<sup>2</sup>) = 6.5 square centimeters (cm<sup>2</sup>)</p> <p>1 square foot (sq ft, ft<sup>2</sup>) = 0.09 square meter (m<sup>2</sup>)</p> <p>1 square yard (sq yd, yd<sup>2</sup>) = 0.8 square meter (m<sup>2</sup>)</p> <p>1 square mile (sq mi, mi<sup>2</sup>) = 2.6 square kilometers (km<sup>2</sup>)</p> <p>1 acre = 0.4 hectare (he) = 4,000 square meters (m<sup>2</sup>)</p>	<p><b>AREA (APPROXIMATE)</b></p> <p>1 square centimeter (cm<sup>2</sup>) = 0.16 square inch (sq in, in<sup>2</sup>)</p> <p>1 square meter (m<sup>2</sup>) = 1.2 square yards (sq yd, yd<sup>2</sup>)</p> <p>1 square kilometer (km<sup>2</sup>) = 0.4 square mile (sq mi, mi<sup>2</sup>)</p> <p>10,000 square meters (m<sup>2</sup>) = 1 hectare (ha) = 2.5 acres</p>
<p><b>MASS - WEIGHT (APPROXIMATE)</b></p> <p>1 ounce (oz) = 28 grams (gm)</p> <p>1 pound (lb) = 0.45 kilogram (kg)</p> <p>1 short ton = 2,000 pounds (lb) = 0.9 tonne (t)</p>	<p><b>MASS - WEIGHT (APPROXIMATE)</b></p> <p>1 gram (gm) = 0.036 ounce (oz)</p> <p>1 kilogram (kg) = 2.2 pounds (lb)</p> <p>1 tonne (t) = 1,000 kilograms (kg) = 1.1 short tons</p>
<p><b>VOLUME (APPROXIMATE)</b></p> <p>1 teaspoon (tsp) = 5 milliliters (ml)</p> <p>1 tablespoon (tbsp) = 15 milliliters (ml)</p> <p>1 fluid ounce (fl oz) = 30 milliliters (ml)</p> <p>1 cup (c) = 0.24 liter (l)</p> <p>1 pint (pt) = 0.47 liter (l)</p> <p>1 quart (qt) = 0.96 liter (l)</p> <p>1 gallon (gal) = 3.8 liters (l)</p> <p>1 cubic foot (cu ft, ft<sup>3</sup>) = 0.03 cubic meter (m<sup>3</sup>)</p> <p>1 cubic yard (cu yd, yd<sup>3</sup>) = 0.76 cubic meter (m<sup>3</sup>)</p>	<p><b>VOLUME (APPROXIMATE)</b></p> <p>1 milliliter (ml) = 0.03 fluid ounce (fl oz)</p> <p>1 liter (l) = 2.1 pints (pt)</p> <p>1 liter (l) = 1.06 quarts (qt)</p> <p>1 liter (l) = 0.26 gallon (gal)</p> <p>1 cubic meter (m<sup>3</sup>) = 36 cubic feet (cu ft, ft<sup>3</sup>)</p> <p>1 cubic meter (m<sup>3</sup>) = 1.3 cubic yards (cu yd, yd<sup>3</sup>)</p>
<p><b>TEMPERATURE (EXACT)</b></p> <p><math>[(x-32)(5/9)]\text{ }^\circ\text{F} = y\text{ }^\circ\text{C}</math></p>	<p><b>TEMPERATURE (EXACT)</b></p> <p><math>[(9/5)y + 32]\text{ }^\circ\text{C} = x\text{ }^\circ\text{F}</math></p>

## QUICK INCH - CENTIMETER LENGTH CONVERSION



## QUICK FAHRENHEIT - CELSIUS TEMPERATURE CONVERSION



For more exact and or other conversion factors, see NIST Miscellaneous Publication 286, Units of Weights and Measures. Price \$2.50 SD Catalog No. C13 10286

Updated 6/17/98

## **Acknowledgements**

---

The authors wish to acknowledge Amtrak and the following individuals for their technical and logistical contribution to this project:

Mike Trosino, Amtrak

Carl Walker, Amtrak

Matthew Greve, Amtrak

John Kotyla, Amtrak

Michael Tomas, Amtrak

Morgan Reed, Fugro N.V.

Adam Mills, Fugro N.V.

# Contents

---

Executive Summary .....	1
1. Introduction .....	2
1.1 Background .....	2
1.2 Objectives .....	2
1.4 Scope .....	2
1.5 Organization of the Report .....	3
2. Field Data Collection.....	4
2.1 Sensor Setup .....	4
2.2 Test Sites .....	6
2.3 Introducing Changes in the Field .....	9
3. Algorithm Development.....	13
3.1 Spike Change Detection .....	13
3.2 Fastener Change Detection.....	15
3.3 Anchor Change Detection .....	16
3.4 Ballast Change Detection .....	17
3.5 Tie Skew Change Detection .....	17
3.6 Joint Change Detection .....	18
3.7 Rail Stamping Information Detection .....	20
4. Conclusion.....	22
5. Recommendations .....	23
Abbreviations and Acronyms .....	24

## Illustrations

---

Figure 1 – Primary Sensor Configuration.....	4
Figure 2 – Side-Scanning Sensor Configuration .....	5
Figure 3 – Correction for Vehicle Motion .....	6
Figure 4 – Map of Bear Maintenance Facility .....	7
Figure 5 – Dash-cam View from Bear Maintenance Facility.....	7
Figure 6 – Map of Wilmington Maintenance Facility .....	8
Figure 7 – Dash-cam View of Mainline Testing .....	8
Figure 8 – Spike Changes .....	9
Figure 9 – Anchor Changes .....	9
Figure 10 – Fastener Changes.....	10
Figure 11 – Ballast Changes .....	10
Figure 12 – Tie Skew Changes .....	11
Figure 13 – Joint Gap Changes.....	11
Figure 14 – Regions of Interest Containing Heads of Spikes.....	13
Figure 15 – Similarity Between Ballast Particles and Spike Heads .....	14
Figure 16 – Fastener Detection Algorithm .....	15
Figure 17 – Anchor Change Detection .....	16
Figure 18 – Ballast Change Detection Algorithm.....	17
Figure 19 – Tie Skew Change Detection .....	18
Figure 20 – Rail Joint Range Image and Change Detection.....	19
Figure 21 – Rail Stamping Information Detection .....	20
Figure 22 – Impact of Corrosion and Surface Contamination on OCR Results.....	21

## Tables

---

Table 1 – Changes Introduced during Each Inspection Run.....	12
Table 2 – Spike Change Detection Results.....	14
Table 3 – Fastener Change Detection Results .....	16
Table 4 – Anchor Change Detection Results .....	17
Table 5 – Ballast Change Detection Results.....	17
Table 6 – Tie Skew Change Detection Results.....	18
Table 7 – Joint Gap Change Detection Results .....	20



## Executive Summary

---

This report documents the successful demonstration of automated change detection on railroad track. Pavemetrics Systems Inc. performed this research under contract with the Federal Railroad Administration between March and December 2017. The project successfully demonstrated the ability of its Laser Rail Inspection System (LRAIL) to detect changes in fasteners, anchors, spikes, ties, joints, and ballast—as well as record rail stamping information on Amtrak's Harrisburg line.

Pavemetrics' complete multiple inspection can run during both nighttime and daytime conditions. Amtrak field staff introduced a variety of changes between runs to permit run-to-run comparisons. Pavemetrics developed algorithms to interrogate the raw data and highlight changes in tie spikes (addition, removal), rail anchors (addition, removal), rail fasteners (addition, removal), ties (skew angle), rail joints (increasing and decreasing gap), and ballast (addition, removal).

Change detection for small, isolated spike changes was challenging due to the similarity in size and shape of the heads of spikes and ballast particles. While it was possible to detect both added and removed spike conditions, false positives were initially concerned the research team. Filtering to limit change reporting to cases involving changes to at least two adjacent ties resolved this issue.

Rail anchor change detection was successful, detecting both added and removed anchor conditions. Excessive ballast volumes, which resulted in the anchor or tie being covered, negatively impacted the ability to detect changes.

The system detected changes in rail fastener conditions. It highlighted missing and added fasteners. As expected, excessive ballast volumes, which result in the fastener or tie being covered, negatively impacted the ability to detect changes.

Pavemetrics was successful in detecting tie skew angle changes. Researchers also determined it necessary to set a threshold to limit skew angle reporting to cases where at least 50 percent or more of the tie surface was visible (not covered in ballast).

The system also detected differences in rail joint gaps between test runs. The system's sensitivity is high. It detected changes in rail joint gaps due to thermal changes, which demonstrated the need to set meaningful change thresholds to account for normal thermal expansion and contraction of rails.

Researchers found ballast change detection feasible, with both added and removed ballast conditions being detected. The system was also able to flag locations with ballast volumes under or over a user-definable threshold.

Finally, the system detected and interpreted rail manufacturing stamps located on the rail web. Additional work is required to optimize the side-scanning sensor mounting, filtering of erroneous data from rail contaminants and optimizing of optical character recognition algorithms.

As a next step, Pavemetrics recommends more extended field trialing in simulated revenue operation to test the system under in-service conditions and to modify the system for fully automated, and possibly autonomous, operation.

# 1. Introduction

---

The Laser Rail Inspection System (LRAIL) is a rail inspection system based on the principle of laser triangulation which combines pulsed, high-power, invisible laser line projectors and synchronized cameras to capture a high-resolution intensity image and 3-dimensional range profile of the railway track. The system captures a ~3.5-meter-wide scan, including a view of the rails, ties, fasteners, and ballast. For this project, the LRAIL was mounted on a hi-rail testing vehicle and deployed on Amtrak's Harrisburg line to collect 3-dimensional scans.

LRAIL includes a library of computer algorithms designed to make automatic measurements, inventory features, and detect changes in track infrastructure. For this project, Pavemetrics researchers developed and used algorithms to record and detect changes in fasteners, anchors, spikes, ties, joints, and ballast—as well as record rail manufacturing information.

Field validation included comparison of manual inspections with manual inspections considered "ground-truth." The primary outcome of this project was field-validated evidence of the technology's ability to automatically detect rail maintenance issues before they become a threat to safety or operational efficiency.

## 1.1 Background

LRAIL technology is directly applicable to the Federal Railroad Administration Track Division strategic priority of developing track inspection technologies that can detect defects before they become failures in service. This technology could eventually be used as a revenue-speed, "single-pass," inspection solution that simultaneously delivers the advantages of multiple technologies.

## 1.2 Objectives

The objective of this project was to evaluate the potential for this technology to intelligently detect relevant changes in infrastructure and/or unsafe conditions.

## 1.3 Overall Approach

The overall approach for the project involved the deployment of LRAIL in the field to capture 3-dimensional data and the development of algorithms in the office to detect changes in captured data. Computer-detected changes were compared to a manual field inspection (the ground-truth), conducted with the assistance of Amtrak staff. Researchers performed multiple inspection runs with two different sensor configurations and data collected during both daytime and nighttime conditions.

## 1.4 Scope

The research team limited change detection algorithms specifically to the cases of added or removed fasteners, anchors, spikes, ties, joints, ballast, and cases of increase and decrease in joint gap. Although the team changed other conditions in the field, including joint skew, tie cracking, insulator removal, spike height, fastener position, etc., they did not develop algorithms to detect those changes for this specific project. Also, while rail stamping information detection was within the scope of the project, they kept change detection regarding that information

outside of the scope. Lastly, algorithm development focused on change detection in normal track areas and excluded changes in special track work locations such as switches and crossings.

## **1.5 Organization of the Report**

This report is organized into five sections. [Sections 2](#) and [3](#) document the field testing and algorithm development. Conclusions are discussed in [Section 4](#) and recommendations for continued research are provided in [Section 5](#).

## 2. Field Data Collection

---

The following sections describe the equipment and activities associated with the field data collection testing on Amtrak.

### 2.1 Sensor Setup

During the data collection phase, Pavemetrics brought a hi-rail vehicle equipped with LRAIL sensors and associated hardware to Amtrak's facility for testing. The hardware package included a wheel-mounted encoder (for distance measurement), a GPS receiver, a DC to AC power inverter, and an industrial computer. Two different sensor mounting configurations were utilized; a top-down setup, (Figure 1) with one sensor directly over each rail and a two-sensor setup with one sensor above one rail and another sensor scanning the gauge-side face of that same rail (Figure 2).



**Figure 1 – Primary Sensor Configuration**



**Figure 2 – Side-Scanning Sensor Configuration**

The top-down setup was the primary configuration used for the project and for all change detection tasks. The side-scanning setup was specifically used to capture rail stamping on the side of the rail, and was not used for change detection.

### ***Motion Compensation***

An inertial measurement unit is enclosed in each sensor head and used to track small changes in the pitch, roll and heading for each sensor. These orientation data were later used by a computer algorithm to remove vehicle motion artifacts from 2-dimensional and 3-dimensional data ([Figure 3](#)).

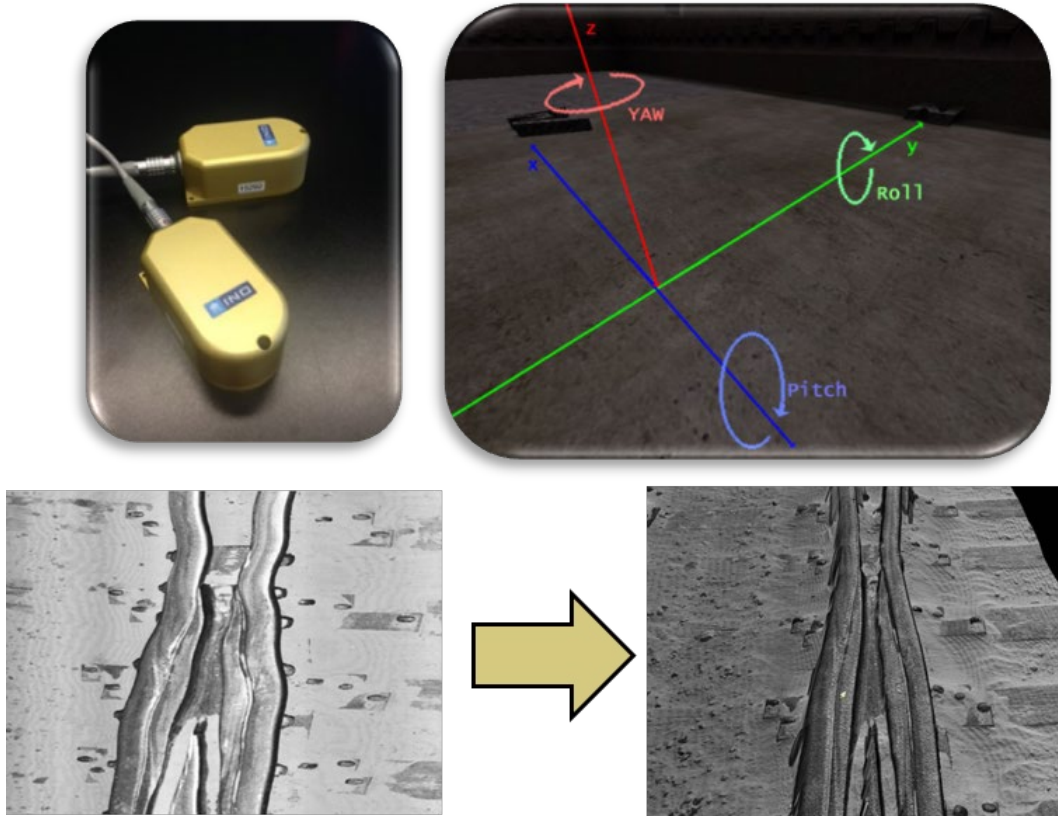


**Figure 3 – Correction for Vehicle Motion**

## **2.2 Test Sites**

Field testing was performed in June 2017 at Amtrak's Bear Maintenance Facility in Delaware. This facility was selected for a variety of reasons, including:

- Ease of track access and generally low track traffic conditions
- The ability to make changes to the track conditions without interrupting normal traffic.
- The flexibility to adjust sensor mounting and system parameters while on-track.

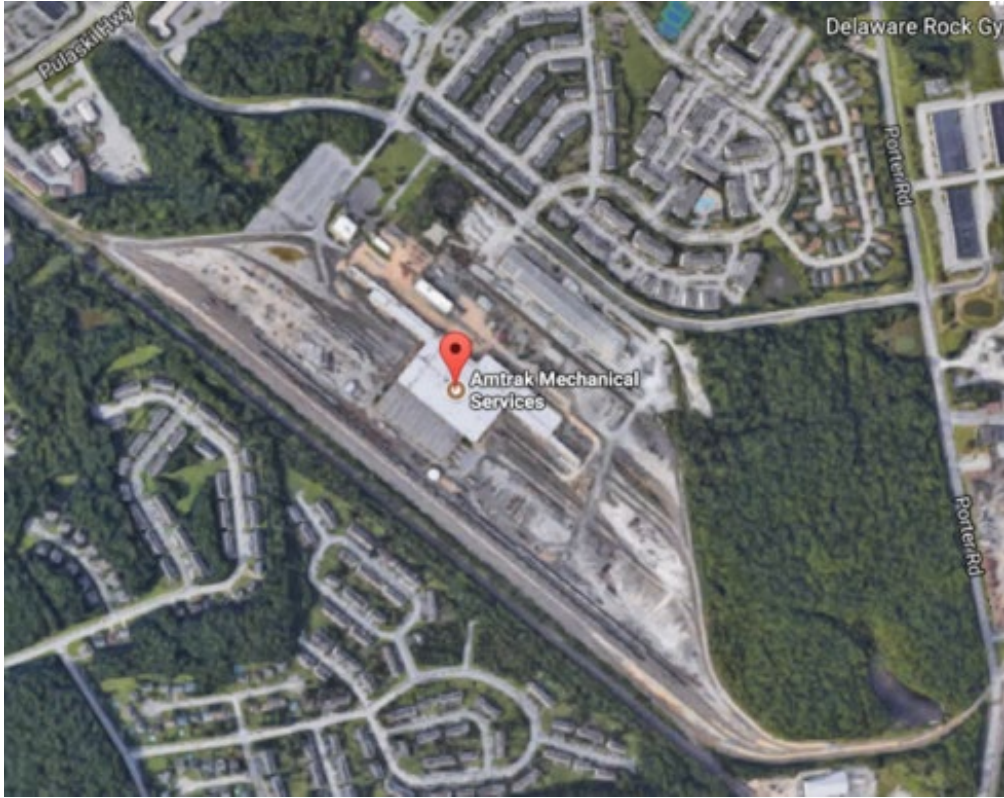


**Figure 4 – Map of Bear Maintenance Facility**



**Figure 5 – Dash-cam View from Bear Maintenance Facility**

Testing was also performed on the mainline near the Wilmington Maintenance Facility, also in Delaware, during off hours to minimize impact to the network.



**Figure 6 – Map of Wilmington Maintenance Facility**



**Figure 7 – Dash-cam View of Mainline Testing**

Once the hi-rail truck was set on the tracks, the LRAIL system parameters were configured and a system calibration was performed before capturing multiple repeat runs. Data collection was performed in accordance with Amtrak rules and regulations.



**2.3 Introducing Changes in the Field**

To test the detection sensitivity of the LRAIL system, a variety of changes were made to assets in the field, including spikes, anchors, fasteners, ballast, tie-skew, and joints. These changes are shown in the following figures.



**Figure 8 – Spike Changes**



**Figure 9 – Anchor Changes**



**Figure 10 – Fastener Changes**



**Figure 11 – Ballast Changes**



**Figure 12 – Tie Skew Changes**



**Figure 13 – Joint Gap Changes**

A total of 16 inspection runs, grouped into 4 sets (Runs 1-7, Runs 8-10, Runs 11-13 and Runs 14-16), were performed at the Bear Yard site. Physical changes were made to track conditions between each set of the runs. All activities were recorded in a log. This approach enabled both modeling of run-to-run consistency when conditions had not been deliberately changed as well as comparison between runs when conditions were deliberately changed.

A summary of the changes made during each set of runs is presented in [Table 1](#).

**Table 1 – Changes Introduced during Each Inspection Run**

<b>Location from Reference Point (feet)</b>	<b>Conditions for Runs 1-7</b>	<b>Conditions for Runs 8-10</b>	<b>Conditions for Runs 11-13</b>	<b>Conditions for Runs 14-16</b>
102			6 anchors installed	2 anchors removed
134			7 spikes removed and 1 installed	
141	Joint closed with putty	Putty removed		
147		1 spike added		
209		Ballast removed		
213		2 anchors installed	2 anchors removed	
218	Joint closed with putty	Putty removed		
227	1 spike installed	1 spike removed		
451			Joint closed with putty	Putty removed
485		Pandrol removed	Pandrol installed	
590		Ballast added to empty cribs		
594		Ballast added to empty cribs		
628		Ballast added to empty cribs		
665		Clip installed		
768			Tie skew angle changed by 2 degrees	
768			Ballast added to empty cribs	

### 3. Algorithm Development

---

The following sections describe the data processing and analysis activities.

#### 3.1 Spike Change Detection

The change detection process involves first detecting the ties and rails, and then defining four regions of interest (ROI) at each intersection point (two on the gauge side and two on the field side). Each ROI was then inspected for the presence of spike heads using a 3-dimensional model (Figure 14). Spike count and average spike height was reported for each ROI and run-to-run comparison was performed on those same metrics.

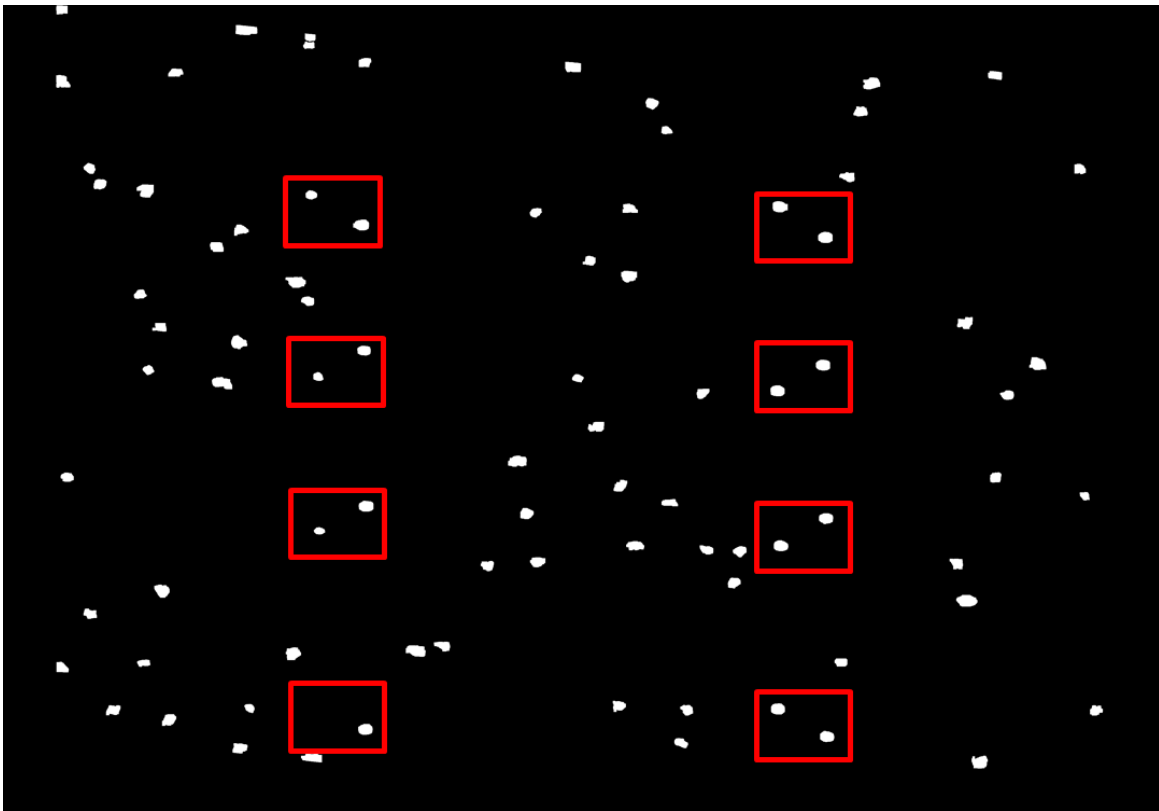


**Figure 14 – Regions of Interest Containing Heads of Spikes**

There was a similarity in size and shape between ballast particles and spike heads (Figure 15) that required the use of a high threshold for comparing candidate spikes against the 3-dimensional model for a genuine spike—to avoid erroneously labeling ballast particles in the ROI as spikes.

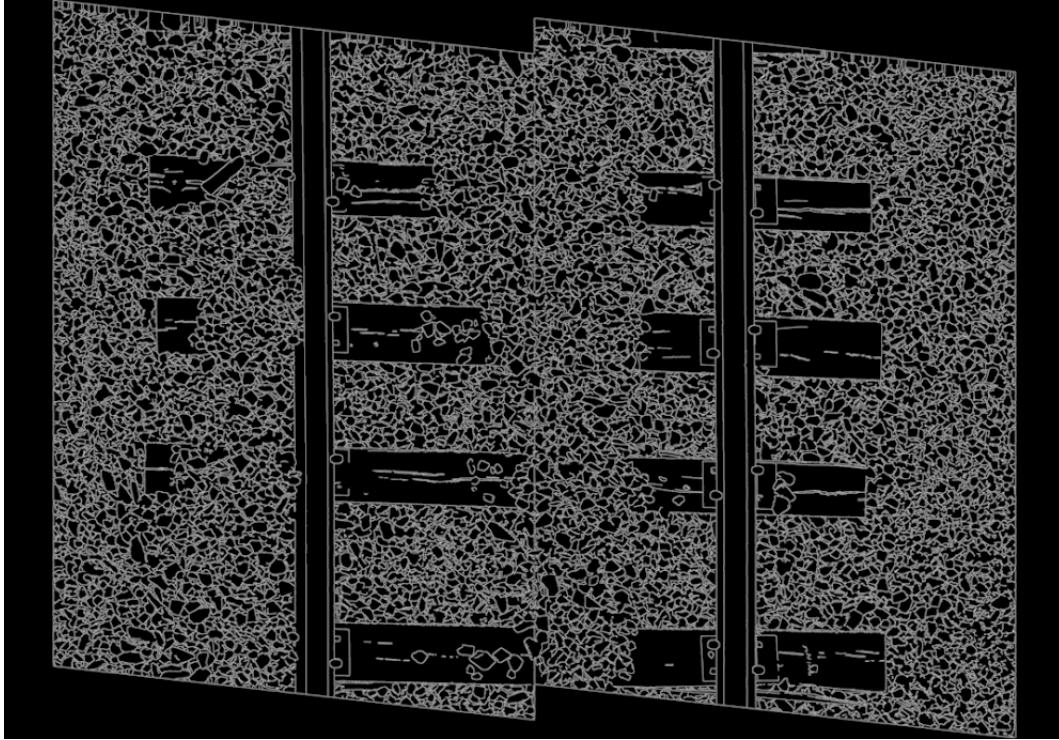


**Figure 15 – Similarity Between Ballast Particles and Spike Heads**

There was a tendency for the system to inconsistently detect spikes near the threshold value and generate a false change. These false positives were eliminated by applying a filter to limit change reporting to cases involving a minimum of two adjacent ties.

The ground-truth for spike detection included the addition and removal of spikes as well as the raising and lowering of spikes. However, change detection for this project was primarily focused on detecting added or removed spikes. Ground-truth examples consisted of small, isolated cases of change (one or two spike changes made on a single tie) instead of a series of changes being made to adjacent ties (e.g., removing spikes from three or four ties in a row). This design was challenging for change detection, and may not reflect a detection condition of high value to a field inspector. In future testing this study recommends changing spikes on a series of adjacent ties.

The change detection algorithms detected the addition and removal of spikes in two or more adjacent ties. The results are presented in [Table 2](#).

**Table 2 – Spike Change Detection Results**

<b>Description of Ground-truth</b>	<b>False Positives</b>	<b>False Negatives</b>
There were three ties upon spikes were added and one tie where spikes were removed.	Zero false positives were reported.	Zero false negatives were produced; 100% of the introduced changes were detected.

### 3.2 Fastener Change Detection

The change detection process first detects the ties and rails, and then defines four regions of interest (ROI) at each intersection (two on the gauge side and two on the field side). Each ROI is then inspected for the presence of fasteners using a three-dimensional model. The status of each ROI was reported in three states: a) fastener present, b) ROI contained an object that resembles a fastener, and c) ROI was empty (Figure 16).

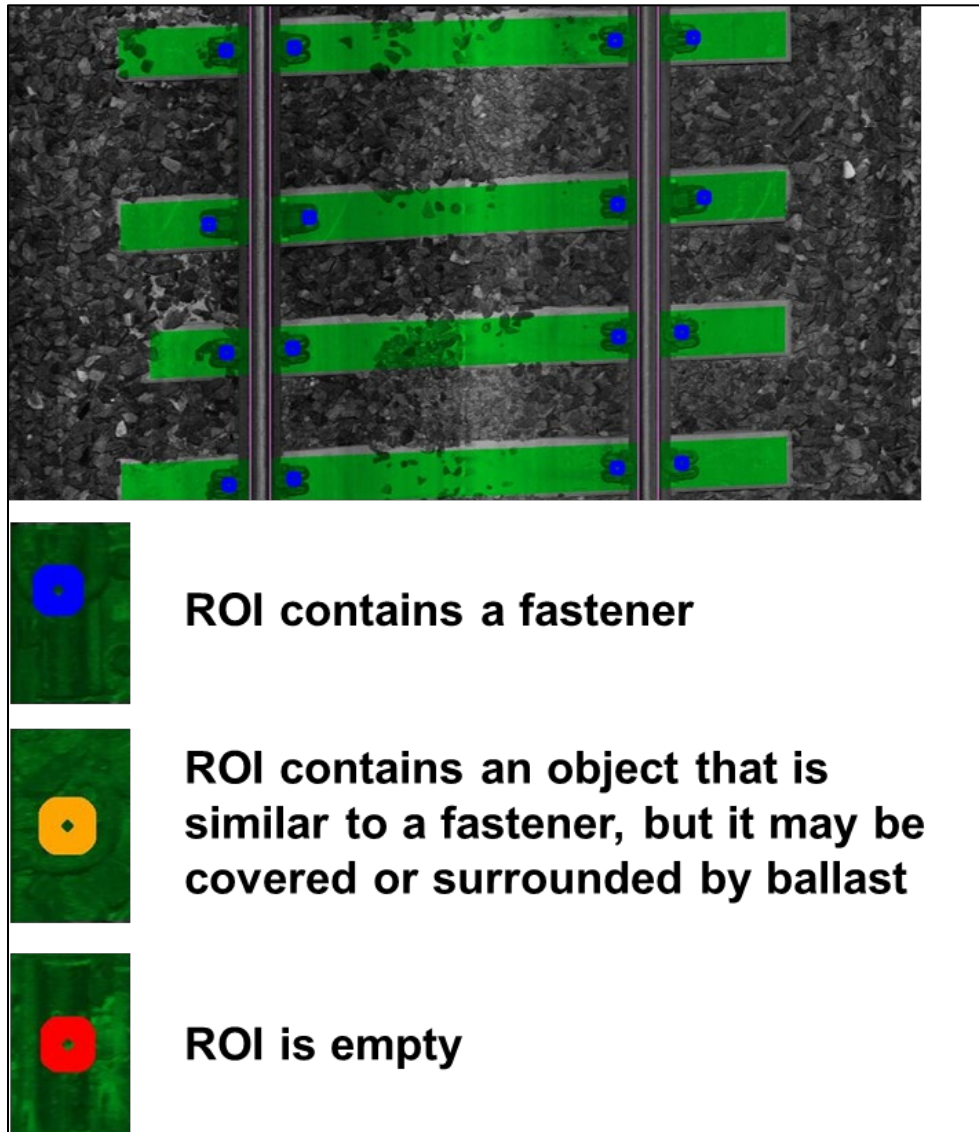


**Figure 16 – Fastener Detection Algorithm**

Filtering was applied to report fastener changes only for cases where two or more adjacent ties contained changes. Ground-truth examples consisted of isolated cases of change (one or two fasteners on a single tie), instead of a series of changes being made to adjacent ties. Change detection was found to be feasible for the detection of added and removed fasteners. Results for fastener change detection are presented in Table 3.

**Table 3 – Fastener Change Detection Results**

Description of Ground-truth	False Positives	False Negatives
There were two cases of fasteners being removed or added.	Zero false positives were reported.	Zero false negatives were produced; 100% of the introduced changes were detected.

### 3.3 Anchor Change Detection

For change detection of anchors, each ROI was inspected for the presence of anchors using a 3-dimensional model before a run-to-run comparison was completed to detect changes (Figure 17).

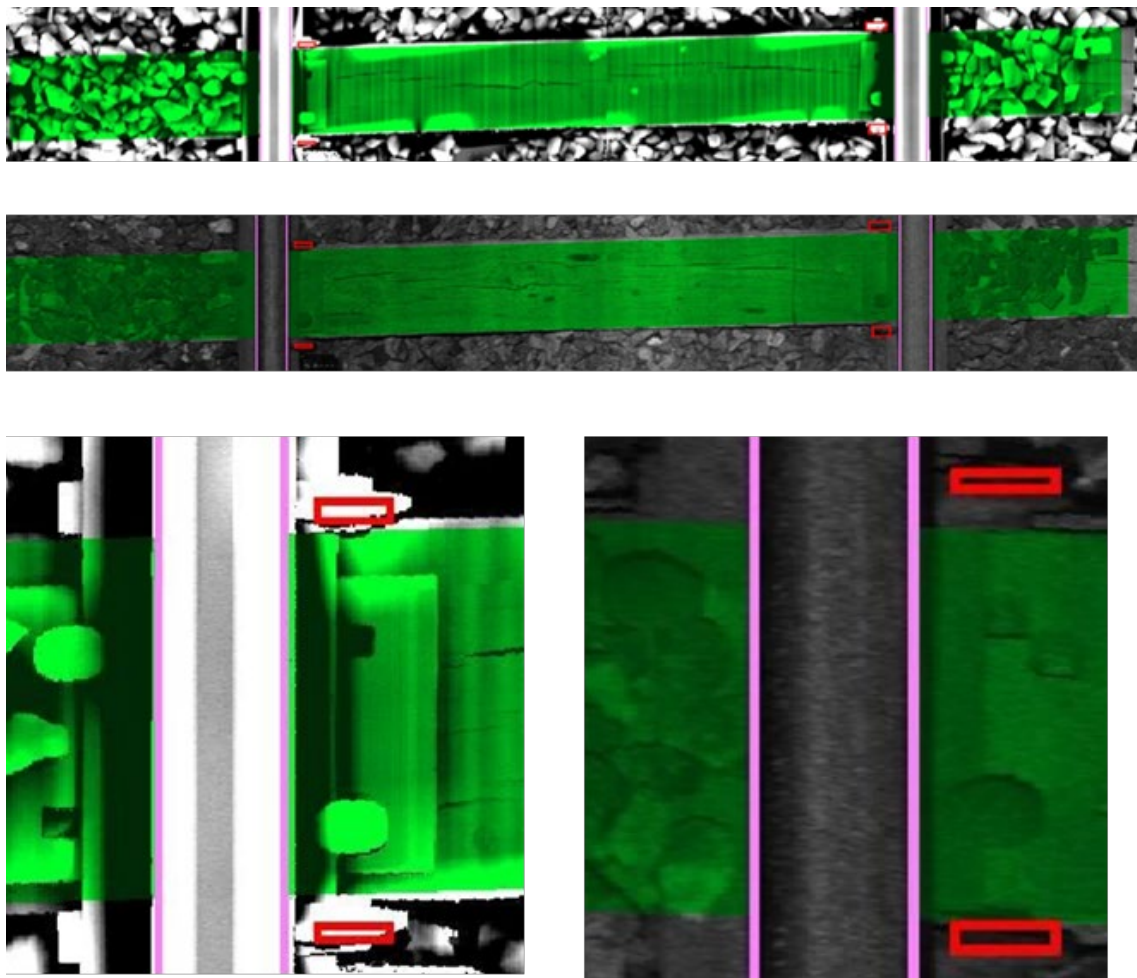


**Figure 17 – Anchor Change Detection**

Ground-truth examples consisted of isolated cases of change (one or two anchors on a single tie) instead of a series of changes being made to adjacent ties. Change detection was found to be feasible for the detection of added and removed anchors. Results for anchor change detection are presented in Table 4.



**Table 4 – Anchor Change Detection Results**

<b>Description of Ground-truth</b>	<b>False Positives</b>	<b>False Negatives</b>
There were three cases of anchors being added.	Zero false positives were reported.	Zero false negatives were reported; 100% of the introduced changes were detected.

### 3.4 Ballast Change Detection

The ballast change detection process involved first detecting the rails to use as a reference point and then measuring ballast volume in relation to the position of the rails. Run-to-run comparison was then performed to flag changes. The program included a user-definable ballast volume threshold (Figure 18).

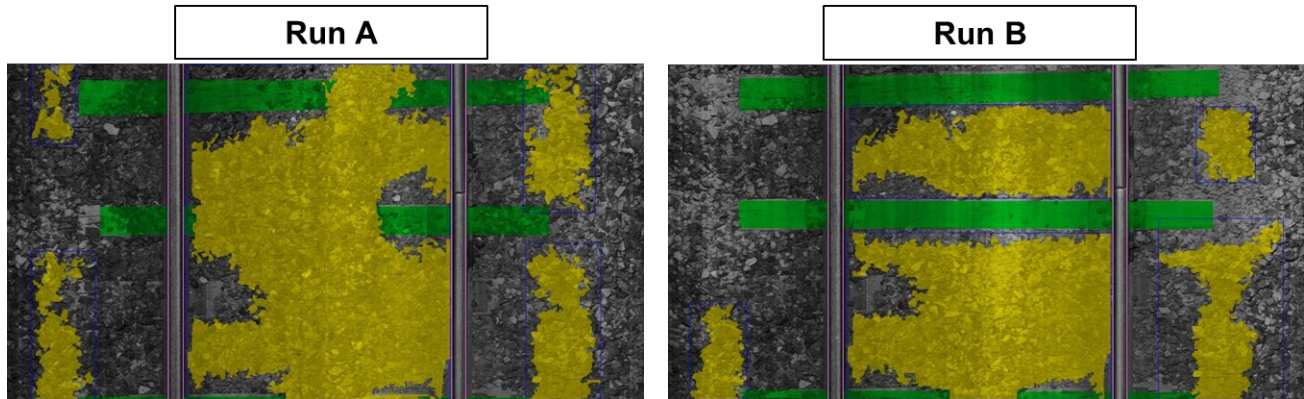


**Figure 18 – Ballast Change Detection Algorithm**

Ground-truth examples included both adding ballast as well as removing ballast. Change detection was found to be feasible for both conditions. Results for ballast change detection are presented in Table 5.

**Table 5 – Ballast Change Detection Results**

<b>Description of Ground-truth</b>	<b>False Positives</b>	<b>False Negatives</b>
There were two locations where ballast was added and two locations where it was removed.	Zero false positives were reported.	Zero false negatives were reported; 100% of the introduced changes were detected.

### 3.5 Tie Skew Change Detection

The tie skew change detection process involved first detecting the ties and rails. A bounding box was then drawn around the detected tie and the angle of the bounding box compared to the angle of the rails. Run-to-run comparison was then used to detect changes (Figure 19).

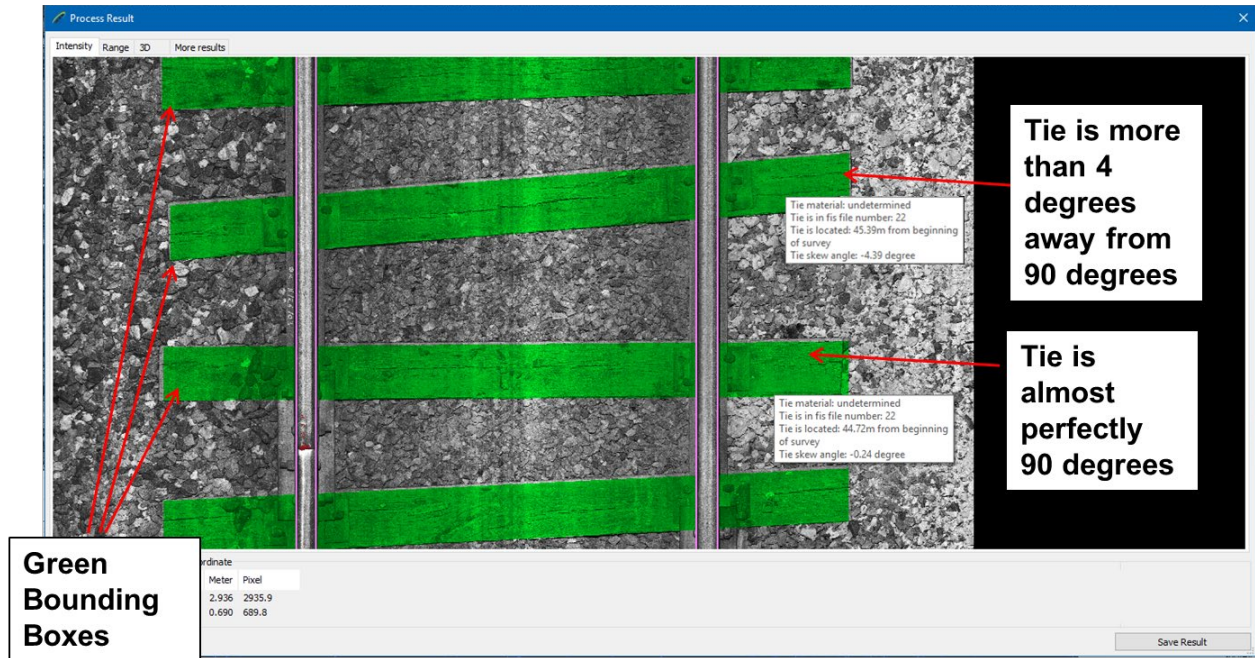


**Figure 19 – Tie Skew Change Detection**

Small changes in skew angle between runs were observed for ties which were significantly covered by ballast, so filtering was applied to report skew angle changes only for ties with at least 50 percent of their surface visible. Ground-truth consisted of a single change where the skew angle of a tie was increased from approximately 90 degrees to approximately 93 degrees. Change detection was found to be feasible, and results are presented in [Table 6](#).

**Table 6 – Tie Skew Change Detection Results**

Description of Ground-truth	False Positives	False Negatives
There was a single location where a tie skew was increased from approximately 90 degrees to approximately 93 degrees.	Zero false positives were reported.	Zero false negatives were produced; 100% of the introduced changes were detected.

### 3.6 Joint Change Detection

The joint change detection process involved first detecting the rails. The longitudinal profile of each rail was analyzed to locate gaps in the rail and joint-gap range images were produced for each location. Finally, a run-to-run comparison was then used to detect changes between runs ([Figure 20](#)).



**Figure 20 – Rail Joint Range Image and Change Detection**

Ground-truth consisted of a total of four cases. Three cases included a joint-gap increase and one case used a gap decrease. Changes were simulated by adding or removing putty from joints. All four change conditions were detectable, but the simulation method was not ideal for a few reasons. First, the putty tended to be displaced from the joint as the inspection vehicle passed the location. This resulted in the reporting of small gaps in joints designed for a zero-gap result. The system reported a gap of a few millimeters versus the expected zero-millimeter result. Second, the putty sometimes produced an abnormal geometry between vertically misaligned rails, which produced unexpected gap measurements. For these reasons, this study recommends not using putty for future testing. Additionally, small changes in gap size due to changing thermal conditions at the test site were also detected, but these results were filtered by applying a 4-mm gap width threshold. Change detection results for joint-gap are presented in [Table 7](#).

**Table 7 – Joint Gap Change Detection Results**

Description of Ground-truth	False Positives	False Negatives
Ground-truth consisted of a total of four cases with three cases involving a joint gap increase and one case involving a decrease in gap.	Zero false positives were reported.	Zero false negatives were produced; 100% of the introduced changes were detected.

### 3.7 Rail Stamping Information Detection

For rail stamping detection, Canny edge detection was used to extract the outline of rail stamping information from range data and an optical character recognition (OCR) algorithm is used to transform shapes into letters and numbers (Figure 21).

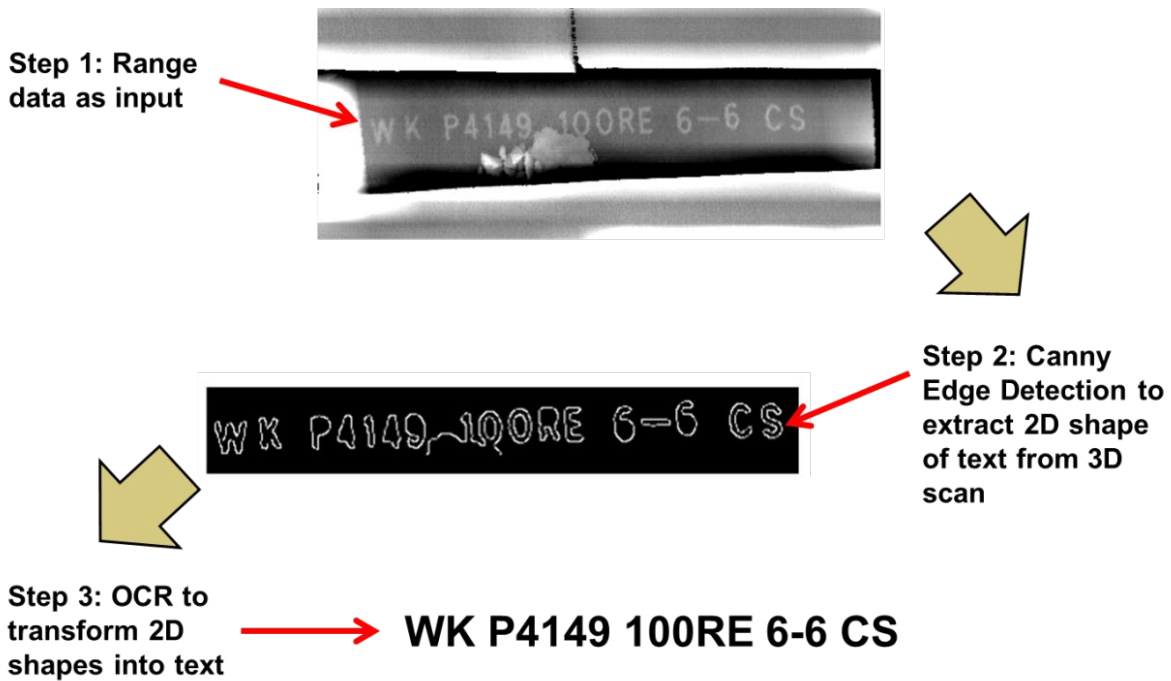
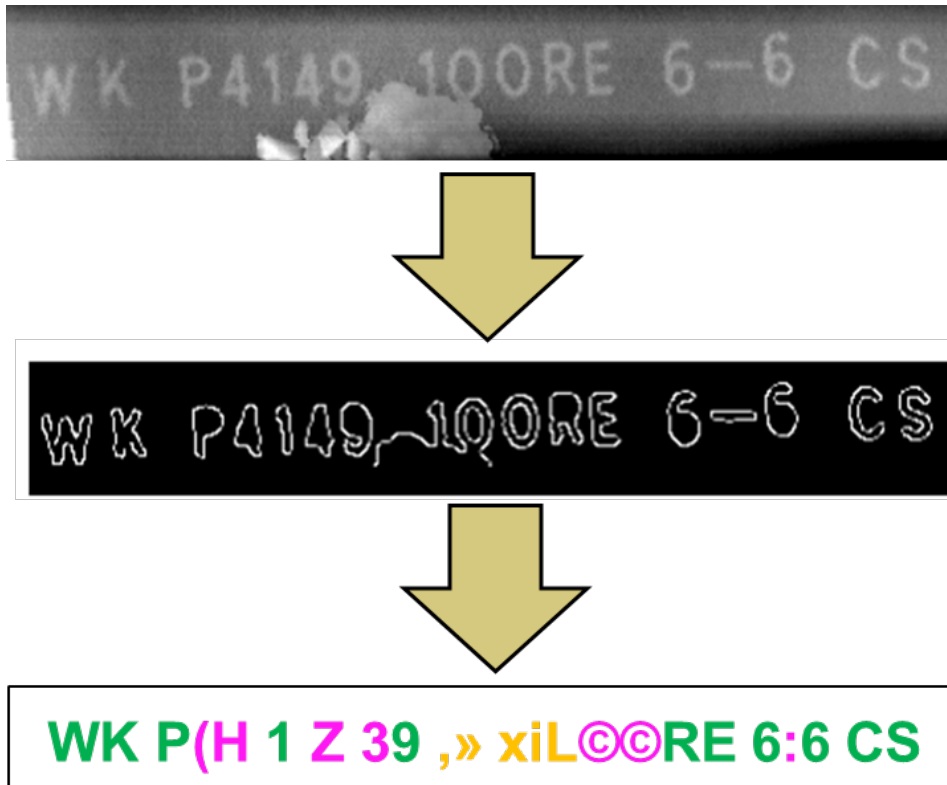


**Figure 21 – Rail Stamping Information Detection**

Range data from both the top-down and side-scan sensor configurations were analyzed. In general, the results showed promise. It was possible to extract reasonable shapes from range data and to translate shapes into characters using OCR. However, surface corrosion and contamination affected the system’s accuracy. Both conditions contributed poor edge detection as well as poor OCR results (Figure 22).



Good edges and good OCR  
 Good edges but poor OCR  
 Poor edges and poor OCR (contaminants)

**Figure 22 – Impact of Corrosion and Surface Contamination on OCR Results**

These results could be improved by filtering the Canny edge detection image to remove the outline of contaminants and by using an improved OCR algorithm. Researchers determined that the side-facing sensor setup was not ideally positioned to capture high-quality range data. The top-scanning equipment performed better. The stamping was clearly visible in range and intensity data from the top-scanning equipment and could be processed by OCR, while the side-scan data sets were poorly resolved.

## 4. Conclusion

---

In this early experimental study, laser triangulation and 3-dimensional analysis technologies were found to be feasible for railway change detection. The following summary conclusions are presented to describe the performance of the system:

- Isolated spike change detection was feasible, but difficult. The similarity in size and shape of the head of spikes to ballast particles and the over-abundance of ballast in the test site (a maintenance yard) resulted in false positives. These false positives were eliminated by applying a filter to limit change reporting to cases involving a minimum of two adjacent ties.
- Fastener change detection was feasible. Added and removed fastener conditions were detected. However, changes in fastener count between runs were observed for ties significantly covered by ballast. Filtering was applied to limit change reporting to cases involving a minimum of two adjacent ties.
- Anchor change detection was feasible. The system correctly reported added and removed anchors.
- Ballast volume change detection was feasible. This system correctly reported locations with added and removed ballast. The system could flag locations with ballast volumes under or over a user-definable threshold.
- Tie skew angle change detection was feasible. However, it was necessary to set a threshold to limit skew angle reporting to cases where at least 50 percent or more of the tie surface was visible to ensure accurate reporting.
- Joint-gap change detection was feasible. The system detected both increased and decreased joint gaps. The effect of thermal changes in the rail on joint-gap widths demonstrated the need to apply sensible thresholds for change reporting joint-gaps.
- Rail stamping information detection and reporting was feasible. More work is needed to optimize the side-scanning sensor mounting to filter erroneous data resulting from rail contaminants and to optimize the OCR algorithms.

## 5. Recommendations

---

The focus of this project was to explore the potential of the LRAIL technology to detect railway changes. The field testing was limited, and the software development effort was focused on providing proof of concept functionality only. More field trialing in simulated revenue service operation is recommended to better understand how this technology could be deployed by inspectors in a live scenario. To proceed in this manner, the following tasks are recommended:

- Software development to integrate the existing automated, but separate, processing steps into a single unified process.
- Software development to create a more user-friendly user interface which field operators can use to operate the sensors and manage the run-to-run inspection process.
- Additional algorithm development to explore the potential to assess railway crosstie cracking, rail surface damage, and the automated inventory of Positive Train Control devices.

## Abbreviations and Acronyms

---

<b>ACRONYM</b>	<b>EXPLANATION</b>
FRA	Federal Railroad Administration
LRAIL	Laser Railway Inspection System
OCR	Optical Character Recognition
ROI	Regions of Investment